The Astronomical Journal, 134:860–866, 2007 August
© 2007. The American Astronomical Society. All rights reserved. Printed in U.S.A.

MULTISITE OBSERVATIONS OF δ SCUTI STARS 7 AQL AND 8 AQL (A NEW δ SCUTI VARIABLE): THE TWELFTH STEPHI CAMPAIGN IN 2003

L. Fox Machado,[1] E. Michel,[2] F. Pérez Hernández,[3,4] J. H. Peña,[5] Z. P. Li,[6] M. Chevreton,[2]
J. A. Belmonte,[3] M. Álvarez,[1] L. Parrao,[5] M.-A. Dupret,[2] S. Pau,[2]
A. Fernandez,[2] J. P. Michel,[2] R. Michel,[1] and A. Pani[1]
Received 2007 April 19; accepted 2007 May 22

ABSTRACT

We present an analysis of the pulsation behavior of the δ Scuti stars 7 Aql (HD 174532) and 8 Aql (HD 174589), a new variable star, observed in the framework of the STEPHI XII campaign during 2003 June and July; 183 hr of high-precision photometry were acquired by using four-channel photometers at three sites on three continents during 21 days. The light curves and amplitude spectra were obtained following a classical scheme of multichannel photometry. Observations in different filters were also obtained and analyzed. Six and three frequencies have been unambiguously detected above a 99% confidence level in the range 190–300 μHz and 100–145 μHz in 7 Aql and 8 Aql, respectively. A comparison of observed and theoretical frequencies shows that 7 Aql and 8 Aql may oscillate with *p*-modes of low radial orders, typical among δ Scuti stars. In terms of radial oscillations the range of 8 Aql goes from $n = 1$ to 3, while for 7 Aql the range spans from $n = 4$ to 7. Nonradial oscillations have to be present in both stars as well. The expected range of excited modes according to a nonadiabatic analysis goes from $n = 1$ to 6 in both stars.

Key words: δ Scuti — stars: individual (HD 174532, HD 174589) — stars: oscillations — techniques: photometric

1. INTRODUCTION

Stellar oscillations provide a powerful tool for studying the interiors of stars, since the mode frequencies depend on the properties of the star and give strong constraints on stellar models and hence evolution theories. However, the observations of stellar pulsations require extensive data sets in order to achieve accurate frequencies and to avoid the sidelobes in the amplitude spectrum caused by the daily cycle. Great efforts are made to optimize the observational coverage of seismological observations, both from the ground via multisite coordinated campaigns (e.g., STEPHI [Stellar Photometry International; Michel et al. 2000] or Delta Scuti Network; Breger et al. 1999) and from space, where missions like *COROT* (Baglin 2003; Michel et al. 2005) will bring close to 100% observational coverage.

In the last two decades the STEPHI network has been engaged in a long-term program aimed at improving our knowledge and description of the physical processes at work in the interior of δ Scuti stars. In the framework of STEPHI campaigns most of the δ Scuti stars within the Praesepe and Pleiades clusters have been observed (e.g., Álvarez et al. 1998; Hernández et al. 1998b; Fox Machado et al. 2002; Li et al. 2004), and several theoretical interpretations have been realized (e.g., Michel et al. 1999; Hernández et al. 1998a; Fox Machado et al. 2006).

The current campaign was devoted to the field star 7 Aql (HD 174532, SAO 142696, HIP 92501), a δ Scuti variable discovered in a systematic search and characterization of new variables, in preparation for the *COROT* mission (Poretti et al. 2003). The star 7 Aql has been cataloged as an evolved δ Scuti star with a low projected rotational velocity, $v \sin i = 32$ km s^{-1}. This star is located in the H-R diagram ($\log g = 3.8 \pm 0.1$ at $T_{\rm eff} = 7400 \pm 100$ K) in the ambiguous transition phase between core hydrogen burning and thick-shell hydrogen burning. This phase is sensitive to the treatment of the core overshooting process. In addition to this, its low $v \sin i$ value makes it an interesting target for modeling and seismic interpretation, since it restricts the seismic analysis either to a star with an intrinsic low rotational velocity or to a faster rotator with a low inclination *i*-value. For evolved δ Scuti variables a very dense spectrum of excited modes is predicted (Dziembowski & Królikowska 1990).

The star 8 Aql (HD 174589, SAO 142706, HIP 92524) was chosen as a comparison star because it is the only bright star located close enough to 7 Aql to permit simultaneous monitoring with the main target within the field of view of the photometer ($\approx 12' \times 16'$), and before this campaign it was thought to be a constant star (Poretti et al. 2003).

Table 1 shows the main observational parameters corresponding to the target stars as taken from the SIMBAD database operated by CDS (Centre de Données astronomique de Strasbourg) including the parallax measurements of *Hipparcos*. Using these values and a reddening of $E(b - y) = 0.004$ mag (Poretti et al. 2003) we estimate a magnitude $M_v = 1.32 \pm 0.10$ for 7 Aql and $M_v = 1.42 \pm 0.10$ for 8 Aql. The estimated absolute magnitudes are in good agreement with those expected for δ Scuti variables (Rodríguez & Breger 2001). Moreover, according to these magnitudes and color indices ($B - V$) it follows that both stars are located inside the δ Scuti instability strip.

2. OBSERVATIONS

The observations in this campaign were carried out over the period 2003 June 17–July 7. As has been done in previous STEPHI campaigns, we observed from three sites well distributed in longitude around the Earth: Observatorio de San Pedro Mártir (SPM, operated by Universidad Nacional Autónoma de México), Baja

[1] Observatorio Astronómico Nacional, Instituto de Astronomía, Universidad Nacional Autónoma de México, A.P. 877, Ensenada, BC 22860, Mexico.
[2] Observatoire de Paris, LESIA, UMR 8109, F-92195 Meudon, France.
[3] Instituto de Astrofísica de Canarias, E-38205 La Laguna, Tenerife, Spain.
[4] Departamento de Astrofísica, Universidad de La Laguna, E-38205 La Laguna, Tenerife, Spain.
[5] Instituto de Astronomía, Universidad Nacional Autónoma de México, A.P. 70-264, México, DF 04510, Mexico.
[6] Beijing Observatory, Chinese Academy of Sciences, Beijing, China.

TABLE 1
OBSERVATIONAL PROPERTIES OF THE STARS OBSERVED IN THE STEPHI 2003 CAMPAIGN

Star	HD	HIP	Spectral Type	V	$B-V$	$v \sin i$ (km s^{-1})	Parallax (mas)	M_V
7 Aql	174532	92501	A2	6.9 ± 0.1	$+0.285 \pm 0.009$	32 ± 3	7.70 ± 0.80	1.32 ± 0.10
8 Aql	174589	92524	F2	6.1 ± 0.1	$+0.299 \pm 0.007$	105 ± 11	11.80 ± 0.78	1.42 ± 0.10

NOTE.—These data were taken from SIMBAD database.

California, Mexico; Xing Long Station (XL, operated by the Beijing Observatory), Heibe Province, China; and Observatorio del Teide (OT, operated by the Instituto de Astrofísica de Canarias), Tenerife, Spain. Thus, we are able to limit systematic gaps in the monitoring of the light curves of our target stars, avoiding the formation of strong aliasing through sidelobes of the spectral window in the Fourier spectrum.

Table 2 gives the log of observations. Bad weather conditions at XL did not allow us to get more than three nights of data from this observatory. A total of 183 hr of useful data were obtained during 21 nights of observations from the three sites. The overlapping between observatories was negligible, and the efficiency of the observations was 36% of the cycle, which is typical for a STEPHI campaign.

Four-channel photometers were used at all sites with interferometric blue filters ($\lambda \approx 4200$ Å, $\Delta\lambda \approx 190$ Å). The channels were used to monitor the stars 7 Aql and 8 Aql, and two adjacent sky background positions. At SPM, the fourth channel was used to monitor the star 7 Aql in a yellow filter ($\lambda \approx 5500$ Å, $\Delta\lambda \approx 400$ Å).

The data reduction is similar to that reported in previous STEPHI campaigns (for details, see Álvarez et al. 1998). First, nightly time series corresponding to sky background were subtracted. Then, we computed the magnitude differences 7 Aql − 8 Aql and subtracted from every light curve each night a second-order polynomial. This removed low-frequency trends that could affect the detection of the oscillation modes at higher frequencies. Finally, we joined the data to produce one temporal series. The resulting differential light curves for three selected days are shown in the top panels of Figure 1.

TABLE 2
LOG OF OBSERVATIONS

Day	Date (2003)	HJD − 2,452,800	SPM (minutes)	XL (minutes)	OT (minutes)
1	Jun 17	8	38	...	...
2	Jun 18	9	18	...	...
3	Jun 19	10	386	...	...
4	Jun 20	11	...	...	...
5	Jun 21	12	366	...	...
6	Jun 22	13	359	...	...
7	Jun 23	14	335	223	...
8	Jun 24	15	359	...	297
9	Jun 25	16	419	...	426
10	Jun 26	17	422	...	425
11	Jun 27	18	420	...	441
12	Jun 28	19	369	...	436
13	Jun 29	20	388	...	282
14	Jun 30	21	425	204	44
15	Jul 1	22	199	...	378
16	Jul 2	23	411	...	433
17	Jul 3	24	353	...	443
18	Jul 4	25	...	339	384
19	Jul 5	26	...	...	418
20	Jul 6	27	...	...	444
21	Jul 7	28	...	...	442
Total	...	...	4908	766	5293

NOTE.—The total observing time was 10,967 minutes (183 hr).

Since only a comparison star was considered we also analyzed the light curves of each star separately. The middle and bottom plots in Figure 1 show examples of the individual light curves of 7 Aql and 8 Aql, respectively. Here a second-order polynomial was used for filtering the low-frequency trends, mainly the harmonics of the day. As can be seen in Figure 1, even in the case of nondifferential photometry the oscillations in 7 Aql and 8 Aql are clearly inferred, with the dominant period of 8 Aql longer than that of 7 Aql.

With the data obtained at SPM we produced three additional temporal series, namely, (1) (7 Aql in blue) − 8 Aql, (2) (7 Aql in yellow) − 8 Aql, and (3) (7 Aql in blue) − (7 Aql in yellow). Thus, we are able to search for phase shifts and amplitude ratios between the two stars. In this case the amplitude spectrum has been filtered with a parabola. The additional results obtained with these light curves are presented in § 4.3.

3. SPECTRAL ANALYSIS

The frequency peaks of the light curves considered in § 2 were obtained by performing a nonlinear fit to the data. However, to show the results and obtain initial estimates of the parameters, we have calculated amplitude spectra of the time series by computing iterative sine wave fits (Ponman 1981). The figures discussed here correspond to this method.

The window function of the observations is shown in Figure 2. A 1 day alias of 58% of the main-lobe amplitude is present. The resolution as measured from the FWHM of the main lobe in the spectral window is $\Delta\nu = 0.84$ μHz.

The amplitude spectrum of the differential light curve 7 Aql − 8 Aql is plotted starting in Figure 3 (*top left*) and continues down and to the right. In order to decide which of the peaks present in the amplitude spectrum can be regarded as a signal from the star, we follow Álvarez et al. (1998), where it was shown that 3.7 times the mean amplitude level in the spectrum, calculated in boxes of 100 μHz, can represent very well the 99% confidence level given by statistical tests. Similar criteria were used in early STEPHI articles (e.g., Michel et al. 1992; Fox Machado et al. 2002). This confidence level is plotted as a solid line in Figure 3.

The spectrum is analyzed with a standard prewhitening method such that in each step the frequency peak with the largest amplitude is subtracted from the time series. The frequency, amplitude, and phase of the prewhitening peak are estimated simultaneously with the previously subtracted ones by performing a nonlinear fit to the original light curve. A new amplitude spectrum with all the fitted peaks subtracted from the light curve is obtained, and a new confidence level computed. Applying the method until the whole spectrum is below the 3.7 signal-to-noise ratio (S/N) level, the frequency peaks that are, with a probability of 99%, due to the star's

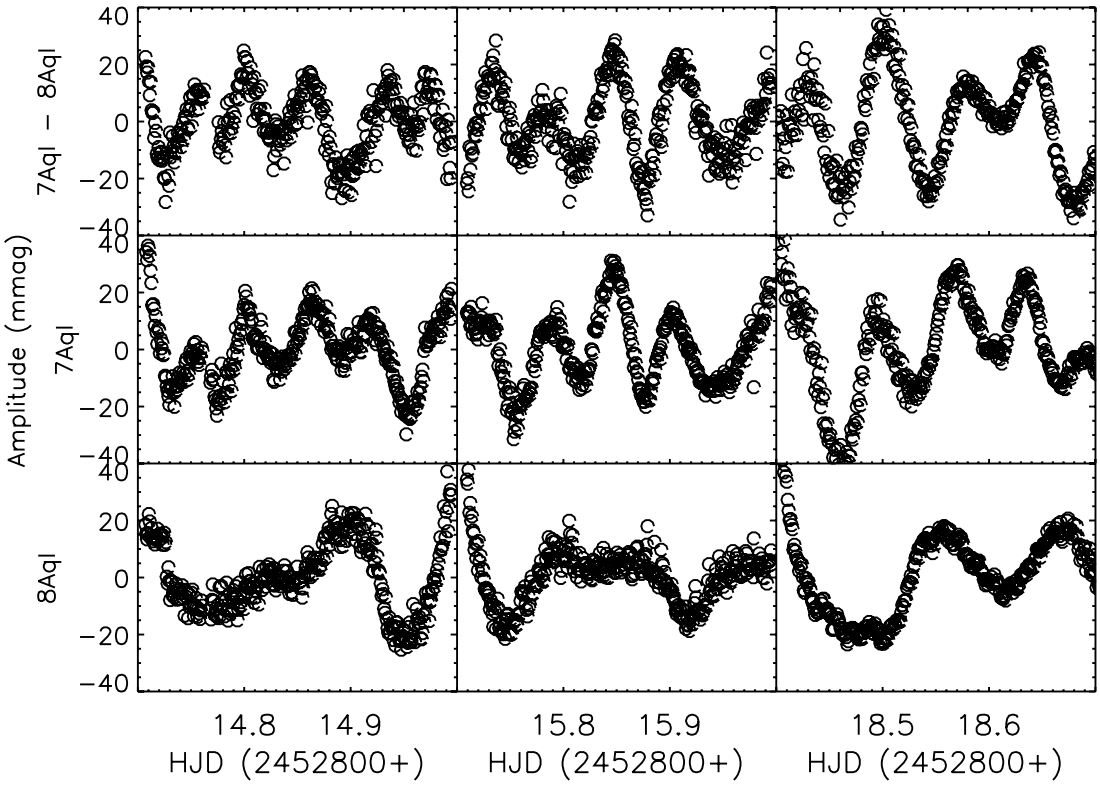

FIG. 1.—Examples of the light curves derived in the framework of the STEPHI XII campaign. Data averaged every 62 s are represented by circles. The three top plots correspond to the differential light curve 7 Aql − 8 Aql, while the middle and bottom plots are light curves for the star indicated in each case. The time series were filtered by a second-order polynomial.

pulsation are obtained. The process is illustrated in Figure 3. It can be seen that the amplitude spectrum of the differential light curve 7 Aql − 8 Aql shows a spread of high-S/N peaks between 80 and 300 μHz. The mean noise level in the amplitude spectrum reaches 580 μmag at 150 μHz and 230 μmag at 400 μHz.

As mentioned earlier, both stars are variable, and hence, it is also necessary to analyze the individual light curves. In order to diminish as much as possible the transparency fluctuations on the nondifferential data we have only considered 18 nights of high photometric quality. During those nights not only were the observing conditions good, but also no pointing and guiding problems were present. A least-squares fit to a parabola was applied and subtracted from every light curve of each of the 18 nights. The resulting amplitude spectra of the nondifferential light curves for 7 Aql and 8 Aql are plotted in Figure 4. The resolution in this case is $\Delta\nu = 1.0$ μHz. The high-S/N peaks are concentrated between 190 and 300 μHz in 7 Aql and between 100 and 170 μHz in 8 Aql. Although the S/N is smaller in these spectra compared to the differential light curve, they are good enough to detect the oscillation frequencies due to each star, as discussed below.

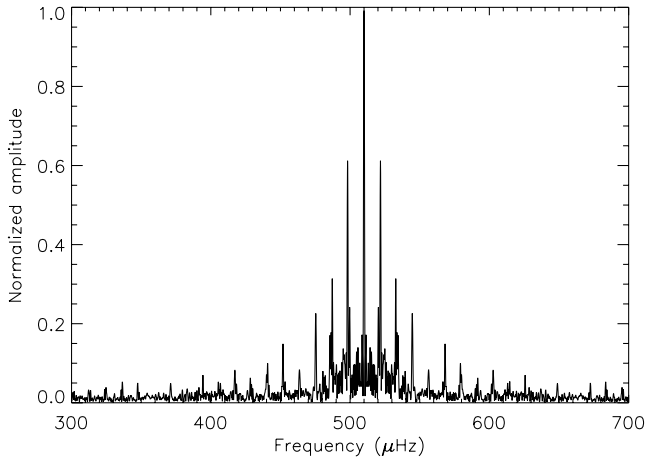

FIG. 2.—Spectral window in amplitude of the STEPHI XII campaign. The first sidelobes are at 58% of the main lobe.

4. RESULTS

4.1. *Detected Frequencies*

The results of the STEPHI XII multisite campaign are summarized in Table 3, where the detected frequencies with their corresponding amplitudes and phases are given. In total nine peaks were detected in the spectrum of the differential light curve; ν_a and ν_b correspond respectively to 5 and 7 cycles day^{-1} and are not considered hereafter.

In order to assign the peaks to a given star, we fit the individual light curves to sinusoidal functions with the frequencies fixed to the values obtained for the differential light curve. These frequencies are marked in Figure 4, and the values of the amplitudes and phases resulting from the fit are given in Table 3, but only for the assigned star. Concerning this point, we note that the peaks of ν_2, ν_3 (in 7 Aql), and ν_8 (in 8 Aql) have S/N > 4 as indicated in Table 3 but also have no significant amplitude in the other star's spectrum. Concerning ν_4, ν_6, and ν_9, they have S/N > 3 in the spectrum of 7 Aql and S/N ≤ 1.6 in the other. On the other hand, the phases are in good agreement with those of the differential light curve.

Since they are hidden in the noise, ν_1, ν_5, and ν_7 can be a little more problematic. For ν_1 and ν_5 the facts that the phases agree

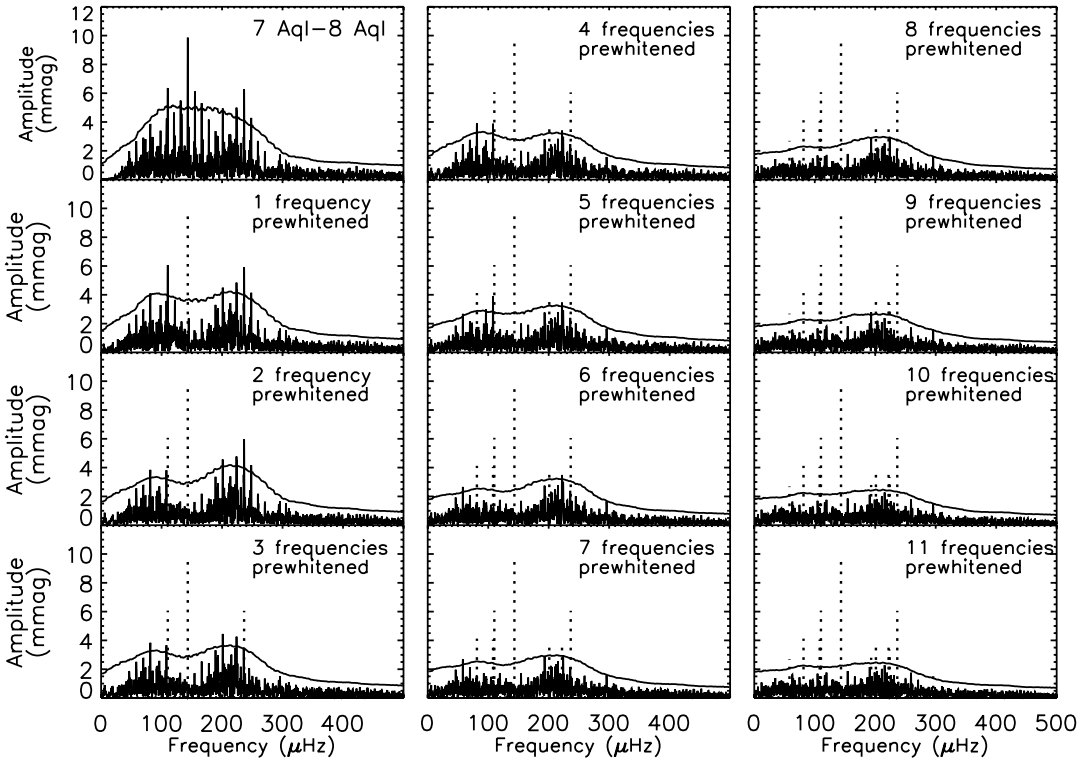

FIG. 3.—Prewhitening process in the spectrum 7 Aql − 8 Aql. In each panel, from top to bottom, one peak above the confidence level (*solid line*) is selected and removed from the time series, and a new spectrum is obtained. In each spectrum, the prewhitened frequencies are shown with vertical dotted lines. The confidence levels are computed as indicated in the text.

with that of the differential data in one of the individual light curves and also that the signal in the other spectrum at those frequencies has S/N $\sim$ 1 makes the identification secure.

As can be seen in Figure 3 the peaks ν_6 and ν_7 are a close frequency pair in the spectrum of the differential light curve. The existence of a residual frequency above the 99% level, when one of them is removed during the prewhitening process (see Fig. 3), gives some confidence that this pair of close oscillation frequencies is indeed intrinsic. In fact, they have a separation of 1.03 μHz above the resolution limit (0.84 μHz). We assigned ν_7 to 7 Aql because its phase in the spectrum of 7 Aql is in good agreement with that of the differential curve, in particular if one notes that both peaks ν_6 and ν_7 are close enough to each other to produce a beating phenomena.

From this analysis it follows that the frequency spectra of both stars are not superposed. The six frequencies of 7 Aql are in the frequency range 195–300 μHz and have amplitudes from 3 to 6 mmag. On the other hand the three peaks detected in 8 Aql are in the range 100–140 μHz and have amplitudes from 4 to 10 mmag.

4.2. *Discussion of the Results*

There is little information available in the literature about the oscillation behavior of 7 Aql and 8 Aql. In particular, Poretti et al. (2003) did not find photometric variability in 8 Aql. For 7 Aql they reported a "peak-to-peak" amplitude of 25 mmag. While this has been enough to confirm the δ Scuti–type variability in 7 Aql, the multiperiodicity of these oscillations has been confirmed only in this campaign. From Table 3 it follows that the oscillation periods of 7 Aql and 8 Aql are within those found in other slightly evolved δ Scuti stars observed from the ground by means of multisite networks (e.g., Breger et al. 1999).

4.3. *Observations in Different Filters*

As was explained in § 2, at SPM observatory two-color photometry was introduced in order to test the potential help that this could bring to mode identification. Figure 5 shows the amplitude spectrum in different filters derived at SPM observatory. As is known, observations from a single site yield a worse window function. In particular, at SPM observatory the sidelobes in the window function are at 88% of the main lobe. It is also important to note that at frequencies below 100 μHz these spectra are dominated by the daily aliasing, mainly for the second one, for which we performed differential photometry with two stars in different filters.

In order to determine the differences in amplitude and phase between the different spectra a linear least-squares fit was performed

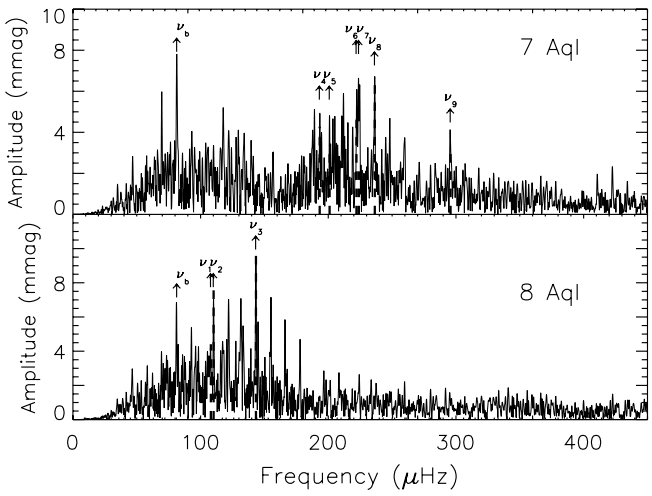

FIG. 4.—Amplitude spectrum derived from individual light curves filtered by a second-order polynomial. The name of the star is indicated in each panel.

TABLE 3
FREQUENCY PEAKS DETECTED ABOVE A 99% CONFIDENCE LEVEL IN THE LIGHT CURVE 7 AQL − 8 AQL

Peak	ν (μHz)	A (mmag)	φ (rad)	S/N
		Differential		
ν_a^*	58.15	2.7	...	...
ν_b^*	81.39	4.1	...	...
ν_1	108.04 ± 0.05	4.1 ± 0.1	−3.12 ± 0.12	6.9
ν_2	110.20 ± 0.01	6.1 ± 0.1	−2.76 ± 0.02	10.2
ν_3	143.36 ± 0.01	9.6 ± 0.1	+2.72 ± 0.01	15.7
ν_4	193.28 ± 0.02	2.8 ± 0.1	−1.53 ± 0.04	4.3
ν_5	201.05 ± 0.01	3.8 ± 0.1	−2.83 ± 0.04	5.6
ν_6	222.08 ± 0.01	3.6 ± 0.1	−2.32 ± 0.04	5.6
ν_7	223.96 ± 0.02	3.4 ± 0.1	+2.30 ± 0.04	5.2
ν_8	236.44 ± 0.01	6.1 ± 0.1	−0.61 ± 0.02	9.9
ν_9	295.78 ± 0.03	1.5 ± 0.1	+1.19 ± 0.08	4.1
		8 Aql		
ν_1	108.04	4.4 ± 0.2	−2.91 ± 0.07	2.2
ν_2	110.20	7.6 ± 0.2	−3.16 ± 0.03	5.1
ν_3	143.36	9.8 ± 0.2	+2.81 ± 0.02	7.9
		7 Aql		
ν_4	193.28	3.8 ± 0.2	−1.75 ± 0.05	3.6
ν_5	201.05	3.0 ± 0.2	−2.83 ± 0.07	2.7
ν_6	222.08	4.3 ± 0.2	−1.99 ± 0.05	3.9
ν_7	223.96	2.2 ± 0.2	+2.42 ± 0.05	2.0
ν_8	236.44	5.8 ± 0.2	−0.56 ± 0.04	5.5
ν_9	295.78	2.9 ± 0.2	+1.14 ± 0.09	3.6

NOTES.—The origin of φ is at HJD 2,452,809.71800. Here, "S/N" is the signal-to-noise ratio in amplitude after the prewhitening process. The formal errors derived from the (no-weighting) nonlinear fit are indicated. Also given are the results of the fit to the individual light curves (at fixed frequencies). For the peaks corresponding to the light curve of 8 Aql a phase of π has been added to help the comparison. An asterisk denotes the fifth and seventh harmonic of the day.

to the SPM light curves with the frequencies fixed to the set listed in Table 3. The resulting phase differences and amplitude ratios between curves (7 Aql in blue) − 8 Aql and (7 Aql in yellow) − 8 Aql are listed in Table 4 (cols. [3] and [4]). The given uncertainties correspond to the result of the no-weighting fit. Since these uncertainties usually underestimate the true errors, it is not clear whether the resulting differences between the two filters are real or are an artifact of the bad coverage from a single site. To test this point we have also computed the spectrum of the light curve (7 Aql in blue) − (7 Aql in yellow). In this case, the extinction effects are not properly canceled, and the daily aliasing dominates the spectrum. Even so, we find some stellar signal above the noise, and the results of the linear fit at fixed frequencies are given in Table 4 (cols. [5]–[7]). At least for ν_8 we obtain a significant S/N, hence showing that the differences in amplitude and phase between the filters considered are indeed real. The derived values of amplitude ratios and phase shift are discussed in § 5.

5. COMPARISON WITH THEORETICAL MODELS

In this section we compute a set of representative models for our target stars to perform simple frequency comparisons, which allows us to obtain some insights on their pulsation behavior. The computation of the theoretical evolutionary sequences and the calibration to the Johnson photometric system are explained in Fox Machado et al. (2006). In particular, we used the CESAM evolution code (Morel 1997) with input physics appropriate to δ Scuti

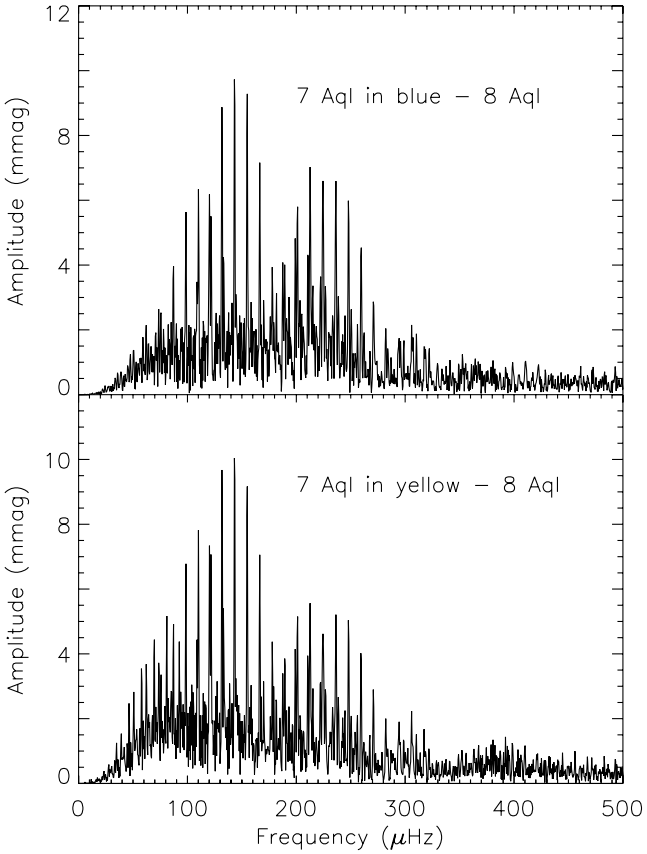

FIG. 5.—Amplitude spectrum derived from SPM light curves in different filters. The names of the curves are indicated in each panel.

stars and with a chemical initial composition of $Z = 0.02$ and $Y = 0.28$. Models with and without convective overshooting have been considered, in the latter case with the parameter $\alpha_{ov} = 0.2$. Rotating evolutionary models were computed just for modeling 8 Aql, since it is a rapid rotator ($v \sin i = 105$ km s^{-1}).

Figure 6 shows the dereddened position of the target stars in a color-magnitude diagram. The slightly brighter star is 7 Aql. The error bars were already given in Table 1 and have been derived using *Hipparcos* data. The dashed and dotted lines are evolutionary sequences of nonrotating models with and without convective overshooting, respectively, giving a range of masses suitable for 7 Aql. The solid lines correspond to evolutionary tracks of rotating models of 2.00 $M_\odot$ (*thin line*) and 2.04 $M_\odot$ (*thick line*), which approximately match the observational position of 8 Aql. In this case, the initial rotational velocity used in each evolutionary sequence (121 km s^{-1} for 2.0 $M_\odot$ and 180 km s^{-1} for 2.04 $M_\odot$) is consistent with the high rotation rate observed in this star. Solid-body rotation with conservation of global angular momentum during the evolution was assumed.

According to the models depicted in Figure 6 our target stars could be in a similar evolutionary stage. In particular, their ages should be between 760 and 1100 Myr with a range of masses of 2.00 ± 0.04 $M_\odot$.

We now use these models to derive a range of radial orders of the target stars. The adiabatic eigenfrequencies were computed using the code FILOU (Tranh Minh et al. 1996; Suárez 2002). As can be seen in Table 3, some of the frequencies of 7 Aql (e.g., ν_1 and ν_2) and 8 Aql (e.g., ν_6 and ν_7) are so close that nonradial oscillations need to be present. This is a common result among δ Scuti stars. However, at the evolutionary stage of our target stars the nonradial oscillation modes develop a mixed character in the

TABLE 4

AMPLITUDE RATIOS A_v/A_y AND PHASE DIFFERENCES $\varphi_v - \varphi_y$ BETWEEN CURVES (7 AQL IN BLUE) − 8 AQL AND (7 AQL IN YELLOW) − 8 AQL

Peak (1)	Frequency (μHz) (2)	A_v/A_y (3)	$\varphi_v - \varphi_y$ (rad) (4)	A_{v-y} (mmag) (5)	φ_{v-y} (rad) (6)	S/N (7)
ν_4	193.28	1.42 ± 0.15	−0.08 ± 0.11	...	...	1.6
ν_5	201.05	0.99 ± 0.08	−0.18 ± 0.08	...	...	1.3
ν_6	222.08	1.07 ± 0.06	+0.01 ± 0.06	...	...	0.5
ν_7	223.96	1.64 ± 0.24	+0.36 ± 0.14	1.31 ± 0.14	+2.66 ± 0.10	2.8
ν_8	236.45	1.25 ± 0.05	−0.01 ± 0.04	1.39 ± 0.11	−0.67 ± 0.08	3.2
ν_9	295.78	1.76 ± 0.13	−0.19 ± 0.08	...	...	2.1

NOTES.—Also shown are the amplitudes, phases, and S/N, obtained from a fit to the light curve (7 Aql in blue) − (7 Aql in yellow). The quoted errors are from the no-weighting least-squares fit.

frequency range of interest, making it difficult to assign radial orders to them without additional constraints. For this reason we prefer to give only the range of n associated with the radial oscillations, keeping in mind that p-modes with $l > 0$ are present as well.

In Table 5 the possible range of radial orders of $l = 0$ modes for the observed frequencies is given. Here we have considered models both with and without convective overshooting. The theoretical frequencies of 8 Aql were computed up to second order in the rotation-rate perturbative treatment. We note that the evolutionary sequences of rotating models with $\alpha_{ov} = 0.2$ are not shown in Figure 6 but were computed with the same masses as indicated by the solid lines. Finally, we have performed preliminary nonadiabatic computations corresponding to our target stars. The nonadiabatic pulsation models considered include the time-dependent convection (TDC) treatment of Gabriel (1996) and Grigahcène et al. (2005). The probable evolutionary stage of the stars is shown in Figure 6. In particular, for 7 Aql we have considered structure models with $M = 2\ M_\odot$, $T_{\rm eff} = 7400$ K, $\log(L/L_\odot) = 1.387$, $X = 0.7$, $Z = 0.02$, $\alpha_{ov} = 0.2$, and different values of the mixing length parameter α (1.8, 1.5, 1, and 0.5).

The stability analysis shows that all the modes in the observed range of frequencies are predicted to be overstable for 7 Aql and 8 Aql. The whole range of predicted overstable radial modes goes from $n = 1$ to $n = 6$.

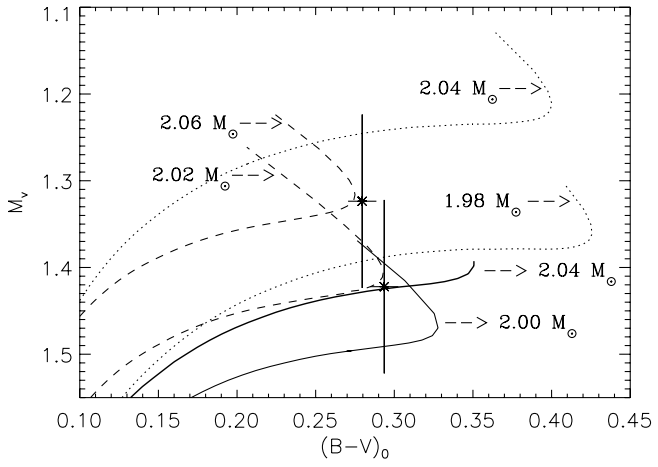

FIG. 6.—Color-magnitude diagram showing the location of the target stars. The slightly cooler star is 8 Aql. Evolutionary sequences of nonrotating models with and without convective overshooting are shown by dotted and dashed lines, respectively. The solid lines are evolutionary sequences of models with no convective overshooting and initial rotation velocities of $v \simeq 121$ km s^{-1} (*thin line*) and $v \simeq 180$ km s^{-1} (*thick line*). The error bars give the positions of the stars according to the uncertainties listed in Table 1.

As shown by Dupret et al. (2005), our TDC treatment allows a much more secure multicolor photometric identification of the degree l of the modes in δ Scuti stars. However, in the case of 7 Aql, the observed error bars on the amplitudes and phases are too large to allow this identification. This is illustrated in Figure 7, where the theoretical amplitude ratios and phases obtained with our TDC treatment for models with different l and α are compared with observations (*large cross*).

6. CONCLUSIONS

We have presented the results obtained in the STEPHI XII multisite campaign. The stars 7 Aql and 8 Aql were monitored for a period of 21 days during 2003 June–July. The analysis reveals that 8 Aql is a new δ Scuti variable.

The three-continent run allowed us to reach a low noise level ($\sim$230 μmag at 400 μHz) and a good spectral window (first sidelobes at 58% of the main lobe in amplitude). The efficiency of the observations was 36% of the cycle. In fact, our campaign represents the most extensive work on 7 Aql and 8 Aql in terms of the time, data points, and observatories involved.

A long differential light curve of 7 Aql−8 Aql was obtained. High-quality photometric nights of data were used to produce a nondifferential time series of each star. We have disentangled the peaks present in each star by comparing the amplitude and phase

TABLE 5

POSSIBLE RANGE OF RADIAL ORDERS OF $l = 0$ MODES FOR EACH OBSERVED FREQUENCY

OBSERVED FREQUENCY (μHz)	n	
	$\alpha_{ov} = 0.00$	$\alpha_{ov} = 0.20$
8 Aql		
$\nu_1 = 108.04$	1, 2	1, 2
$\nu_2 = 110.19$	1, 2	1, 2
$\nu_3 = 143.36$	2, 3	2, 3
7 Aql		
$\nu_4 = 193.29$	4	4, 5
$\nu_5 = 201.05$	4	4, 5
$\nu_6 = 222.08$	5	5, 6
$\nu_7 = 223.96$	5	5, 6
$\nu_8 = 236.45$	6	6, 7
$\nu_9 = 295.78$	7	7

NOTE.—All the models have $Z = 0.02$ and $Y = 0.28$.

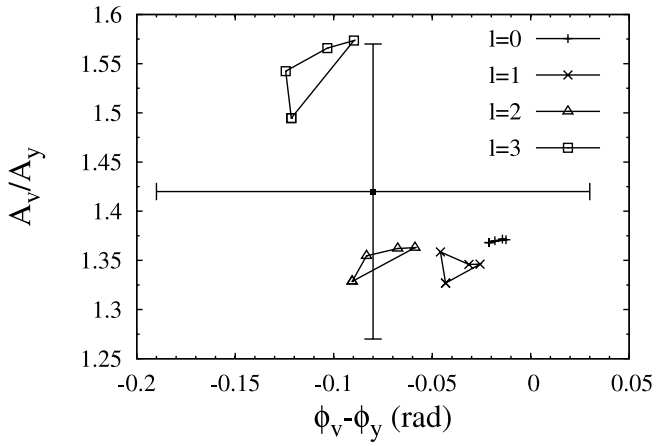

FIG. 7.—Theoretical amplitude ratios and phase differences compared with observations (*large cross*) for the mode ν_4 of 7 Aql. Each group of points related by lines corresponds to a different degree l. Each point of a group corresponds to a model with given α (values: 0.5, 1, 1.5, and 1.8).

values of the nondifferential time series to those of the differential light curve at fixed frequency values. We have found that the frequency spectra of both stars are not superposed. The stars 7 Aql and 8 Aql have been found to be multiperiodic pulsators with at least six and three modes of oscillations, respectively. The resulting amplitude spectra of nondifferential and differential photometry do not shed any doubt on the results. Even so, we are considering new observations involving the faint comparison stars close to 7 Aql and 8 Aql in order to confirm the list of oscillation frequencies by means of ensemble photometry.

A comparison of observed and theoretical frequencies of the radial modes reveals that pulsations in 7 Aql and 8 Aql can be due mostly to low-order p-modes, with radial orders typical among δ Scuti stars. In particular, we have found that the oscillation spectra of 7 Aql and 8 Aql contain frequencies of radial modes with overtones up to $n = 7$ and 3, respectively. Nonradial oscillations must be present in both stars as well. A nonadiabatic analysis shows that the modes in the observed range of frequencies in 7 Aql and 8 Aql are theoretically overstable. The same range of radial orders was expected to be excited in both stars, the opposite of what is found in the observations. In particular, the whole range of predicted overstable radial modes goes from $n = 1$ to 6 in both stars, whereas the observed frequency peaks in each star span over a more restricted range of consecutive radial orders between $n = 1$ and 3 (in 8 Aql) and between $n = 4$ and 7 (in 7 Aql).

This work has received financial support from the French CNRS, the Spanish DGES (AYA 2001-1571, ESP 2001-4529-PE, and ESP 2004-03855-C03-03), the Mexican CONACYT and UNAM under grant PAPIIT IN110102 and IN108106, and the Chinese National Natural Science Foundation under grants 10573023 and 10433010. Special thanks are given to the technical staff and night assistant of the Teide, San Pedro Mártir, and Xing-Long Observatories, and the technical service of the Meudon Observatory. The 1.5 m Carlos Sánchez Telescope is operated on the island of Tenerife by the Instituto de Astrofísica de Canarias in the Spanish Observatorio del Teide. This research has made use of the SIMBAD database operated at CDS, Strasbourg, France. We thank the anonymous referee for helping us to improve the manuscript.

REFERENCES

Álvarez, M., et al. 1998, A&A, 340, 149
Baglin, A. 2003, Adv. Space Res., 31, 345
Breger, M., et al. 1999, A&A, 349, 225
Dupret, M.-A., Grigahcène, A., Garrido, R., De Ridder, J., Scuflaire, R., & Gabriel, M. 2005, MNRAS, 361, 476
Dziembowski, W., & Królikowska, M. 1990, Acta Astron., 40, 19
Fox Machado, L., Pérez Hernández, F., Suárez, J. C., Michel, E., & Lebreton, Y. 2006, A&A, 446, 611
Fox Machado, L., et al. 2002, A&A, 382, 556
Gabriel, M. 1996, Bull. Astron. Soc. India, 24, 233
Grigahcène, A., Dupret, M.-A., Gabriel, M., Garrido, R., & Scuflaire, R. 2005, A&A, 434, 1055
Hernández, M. M., Perez Hernandez, F., Michel, E., Belmonte, J. A., Goupil, M. J., & Lebreton, Y. 1998a, A&A, 338, 511
Hernández, M. M., et al. 1998b, A&A, 337, 198
Li, Z.-P., et al. 2004, A&A, 420, 283
Michel, E., et al. 1992, A&A, 255, 139
———. 1999, A&A, 342, 153
———. 2000, in ASP Conf. Ser. 203, The Impact of Large-Scale Surveys on Pulsating Star Research, ed. L. Szabados & D. W. Kurtz (San Francisco: ASP), 483
———. 2005, in ASP Conf. Ser. 333, Tidal Evolution and Oscillations in Binary Stars, ed. A. Claret, A. Giménez, & J.-P. Zahn (San Francisco: ASP), 264
Morel, P. 1997, A&AS, 124, 597
Ponman, T. 1981, MNRAS, 196, 583
Poretti, E., et al. 2003, A&A, 406, 203
Rodríguez, E., & Breger, M. 2001, A&A, 366, 178
Suárez, J. C. 2002, Ph.D. thesis, Univ. Paris (Denis Diderot)
Tranh Minh, F., et al. 1996, Poster Papers, IAU Symp. 181, Sounding Solar and Stellar Interiors, ed. J. Provost & F.-X. Schmider (Nice: Obs. Cote d'Azur)